Available online at www.sciencedirect.com

ScienceDirect

Procedia Engineering 103 (2015) 657 – 662

Procedia Engineering

www.elsevier.com/locate/procedia

The 13th Hypervelocity Impact Symposium

Ultra-High-Speed Photography and Optical Flash Measurement of Nylon Sphere Impact Phenomena

M. Yanagisawa[a,*], K. Kurosawa[b], and S. Hasegawa[c]

[a]*Univ. Electro-Communications, 1-5-1 Chofugaoka, Chofu-shi, Tokyo 182-8585, Japan*
[b]*Chiba Institute of Technology, 2-17-1 Tsudanuma, Narashino-shi, Chiba 275-0016, Japan*
[c]*Inst. Space Astronaut. Sci., JAXA, Chuo-ku, Sagamihara-shi, Kanagawa 252-5210, Japan*

Abstract

An optical spike is sometimes observed prior to the main flash in high-velocity impact experiments. The spikes are particularly noticeable in the case of Nylon66 projectiles. In this study, we conducted experiments in which Nylon66 spheres impacted the flat surfaces of Nylon66 blocks perpendicularly at 7 km s^{-1}. We observed the impact phenomena by using an ultra-high-speed camera and high-temporal-resolution photometers to identify the cause of the spikes. High-speed photographs show that the entire projectile was shining while it was penetrating a target. Glaring light from the shock front propagating in the projectile is assumed to become diffused within the translucent projectile and then radiated from its surface. The blackbody radiation from the shock front at 3600 K, which is calculated based on a one-dimensional shock model, accounts for the radiative intensities measured by the photometers. A sub-spike was observed just after the main spike in all the experiments conducted, the cause of which was not ascertained.

Peer-review under responsibility of the Curators of the University of Missouri On behalf of the Missouri University of Science and Technology

Keywords: impact flash; high-speed-photograpy; nylon

1. Introduction

Observation of optical flashes is one of the basic tools in the study of high-velocity impact phenomena in laboratory experiments. Jean and Rollins [1] noted that a flash consists of two successive events. The first event, a “spike”, has a duration that is less than the projectile diameter divided by the impact velocity. The second event, a “tail”, is caused by radiation from an expanding jet [1]. They attributed the spike to the initial luminosity at the beginning of the jetting phenomena.

The initiation of a jet, which causes the spike, was studied by Ang [2]. He compared the velocities of shock waves generated for a spherical projectile and for a flat target with the velocity of the intersection of the projectile and target surfaces. The intersection velocity was much faster than the shock velocities initially. A jet then started to be formed when one of the shock wave velocities exceeded the intersection velocity.

Ernst and Schultz [3] conducted impact experiments at 1.6-1.9 km s^{-1} using particulate pumice dust targets and spherical projectiles made of Pyrex glass or aluminum. They observed spikes when Pyrex projectiles hit the targets, but not when aluminum projectiles were used. They concluded that the source of the spike was located at the interface between the penetrating projectile and the target, and its visibility was enhanced due to the transparency of the Pyrex projectile, but muted in the case of the opaque aluminum projectiles.

* M. Yanagisawa. Tel.: +81-42-443-5198; fax: +81-42-443-5291.
E-mail address: yanagi@uec.ac.jp.

Peer-review under responsibility of the Curators of the University of Missouri On behalf of the Missouri University of Science and Technology
doi:10.1016/j.proeng.2015.04.085

7-mm Nylon66 spheres are among the standard projectiles used at the Two Stage Light Gas Gun Facility at ISAS/JAXA (Institute of Space and Astronautical Science/Japan Aerospace Exploration Agency), and many high-velocity impact experiments have been conducted using these projectiles. In experiments where light sensors are used, spikes have been commonly observed. The cause of the spikes may be different from those cited in previous studies [1-3]. We conducted impact experiments to ascertain the origin of the spikes observed in the case of Nylon66 projectiles by using ultra-high-speed photography and high-speed photometry.

2. Experiments

Experiments were conducted at the Two Stage Light Gas Gun Facility at ISAS/JAXA, in which 7-mm Nylon66 spheres were shot against the surface of a Nylon66 block at 7 km s^{-1} on three occasions (Table 1). The blocks, which measure 80 × 80 × 40 mm, are large enough to be considered as half-spaces, and the projectiles struck their flat surfaces perpendicularly. The vacuum degree in the impact chamber was about 10 Pa.

Table 1. Experimental conditions

Shot No.	Impact velocity [km s^{-1}]	Ambient pressure [Pa]	PD lens focal length [mm]	PD lens aperture [mm]	Field of view of PD with lens [mm]
1541	6.987	10.3	8	5.7	820
1544	6.982	13.7	55	31	120
1545	6.987	12.8	55	31	120

Impact flashes were measured using a Si PIN photodiode (Hamamatsu Photonics Inc. S3071 [4]) with an amplifier (Hamamatsu Photonics Inc. C8366 [5]). The photodiode (PD) has a sensitive area 5 mm in diameter. It is most sensitive at 900 nm in wavelength and has a sensitivity between 300 and 1100 nm (Fig. 1). The cutoff frequency of the photodiode-amplifier system is 40 M Hz. We attached camera lenses with the focal lengths and apertures shown in Table 1 to the PD to increase overall sensitivity and limit the field of view. No optical filters were used. The PD system was sited just outside the impact chamber 1310 mm from the targets, and was pointed at the impact points through a transparent chamber window. The line of sight had an angle of 17° with the target surfaces. The field of view at the targets—as calculated from the sensor size, the focal length, and the distance—are shown in Table 1.

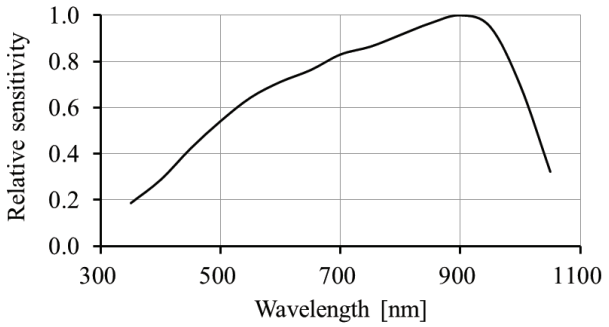

Fig.1. Spectral sensitivity of a Si PIN photodiode (Hamamatsu Photonics Inc. S3071) relative to peak value [4] used in the experiments.

C_2 radicals are generated when Nylon66 is decomposed due to impact. Two avalanche photodiode (APD) modules with optical filters were used to examine the contribution of the C_2 radiation. One APD module (Hamamatsu Photonics Inc. C5331-13 [6]) was fitted with a filter having a peak transmittance at 513 nm in wavelength where strong C_2 radiation exists. The other APD module (Hamamatsu Photonics Inc. C5331-05 [6]) was fitted with a filter having a peak transmittance at 530 nm where no C_2 radiation exists. We refer to the modules with the filters as APD513 and APD530, respectively. Both modules have sensitive areas measuring 5 mm in diameter and their cutoff frequencies are 20 M Hz (APD513) and 50 M Hz (APD530), respectively. The full-width-half-maximum (FWHM) of both the filters is 10 nm in wavelength. No lenses were used, and long hollow cylinders were used to constrain the incident angle of light to the filters to less than 5°. The modules were sited 1550 mm from the targets. Their fields of view of the target—as calculated from the sensor size, cylinder size

and the distance—were 180 mm for a full view and 270 mm for a partial view. Their line of sight had an angle of about 11° with the target surfaces.

An ultra-high-speed camera (NAC Image Technology Inc. ULTRA Neo) was triggered by the PD signal and captured an image every 50 ns (total 12 frames). The field of view of the camera was almost the same as that for the PD with the 55 mm lens. The camera viewed the target surface edge-on.

3. Results

Both the spike and the tail were easily recognized in the record of PD in experiment 1541 (Fig. 2). It should be noted that the radiant intensities shown in our figures I_{PD} are weighted by the relative spectral sensitivity $f(\lambda)$ shown in Fig. 1 as follows:

$$I_{PD} = \int I(\lambda) \cdot f(\lambda) \cdot \mathrm{d}\lambda \tag{1}$$

where $I(\lambda)$ denotes spectral intensities as functions of wavelength λ.

The field of view of the PD was wide enough in this experiment to include all luminous objects within the time range shown in the figure. The temporal variations of the spikes are very similar in all three experiments, though the amplitude is smaller in experiment 1541 than the others by about 25%. This may be due to a possible large error in the lens aperture for experiment 1541.

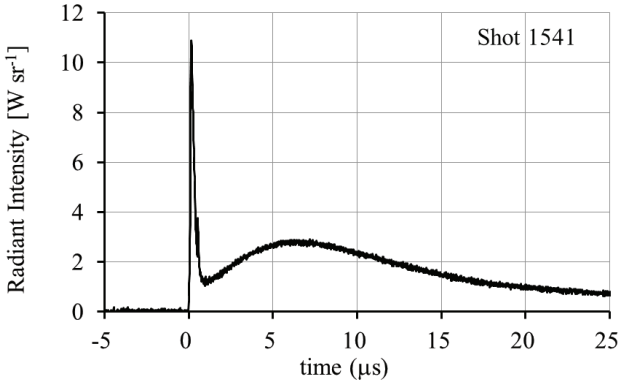

Fig.2. Typical temporal variation of impact flash intensities for Nylon66 spherical projectiles impacting Nylon66 blocks (experiment 1541). The radiant intensity shown here is weighted by the relative spectral sensitivity of the photodiode (Fig. 1). The signal is not saturated at the peak of the spike.

The temporal variation of the spike for experiment 1545 is shown in Fig. 3. The exposure timing signal of the ultra-high-speed camera is also shown in the figure. It should be noted that a sub-spike at t = 0.52 μs was observed in all three experiments. Figure 4 shows camera frames corresponding to the exposure numbers in Fig. 3. Only the central portion of each frame is displayed. One can clearly see a shining projectile penetrating into the target. The expansion of jetting materials is also seen in the frames, but they are not as bright as the shinning projectile.

Figure 4 includes the results of a numerical simulation made using AutoDyn software (ANSYS Inc.), in which pressures are represented by color scales. The linear relations between particle velocity u_p and shock velocity U_s, $U_s = C_0 + su_p$ were used in the simulations, where C_0 and s were, respectively, 2.40 km s^{-1} and 1.91 for u_p < 2 km s^{-1}, and 3.88 km s^{-1} and 1.17 for u_p > 2 km s^{-1}. These values are consistent with the experimental data edited by Marsh [7]. The projectile is 7 mm in diameter and 7 km s^{-1} was the initial velocity in the simulation, and each frame from the ultra-high-speed camera is compared with the simulation result at equivalent time steps (there is 0.05 microsecond between frames). It should be noted that the shock-compressed region in the projectile does not expand above the target surface.

Spectral intensities were obtained by APD513 and APD530 for experiment 1545 and the intensity ratios between the two wavelengths are shown in Fig. 5. The ratio increases significantly after the spike, showing the contribution of C_2 in the tail due to the jetting. In other words, the small ratio at the spike indicates its spectrum is more dominated by the continuum than the tail. The spectra obtained by a high-speed spectrometer in experiments 1544 and 1545 in the wavelength range of 370-720 nm also show that the continuum is more important in the spike than in the tail (Kurosawa personal communication).

The impact crater formed in experiment 1545 is shown in Fig. 6. The impacts significantly fragmented the blocks, but craters were always preserved on one of the largest fragments in our experiments, the inner walls of which were covered with impact melts. Shock heating may reduce the brittleness and increase the toughness of Nylon66, and it then may become more resistant against fragmentations due to the rarefaction waves and stress waves that follow. The numerical simulations using AutoDyn were stopped before the final craters were formed. Therefore, we cannot compare the crater sizes and shapes between the experiments and the simulations.

4. Discussion

Figure 4 clearly shows that the spike radiation mainly originates from the penetrating projectile. The radiation from the shock-compressed high-temperature region, located below the target surface (see the lower panel of Fig. 4), is assumed to be emitted through the translucent Nylon66 projectile. The initial luminosity at the beginning of the jetting phenomena proposed by Jean and Rollins [1] may also exist, but it is not a dominant component in the case of translucent projectiles. There may be emissions through the translucent Nylon66 target. Their contributions are not important, however, because radiation is absorbed as well as scattered while traveling through the target, which was large, and because our instruments observed the target surface nearly edge-on.

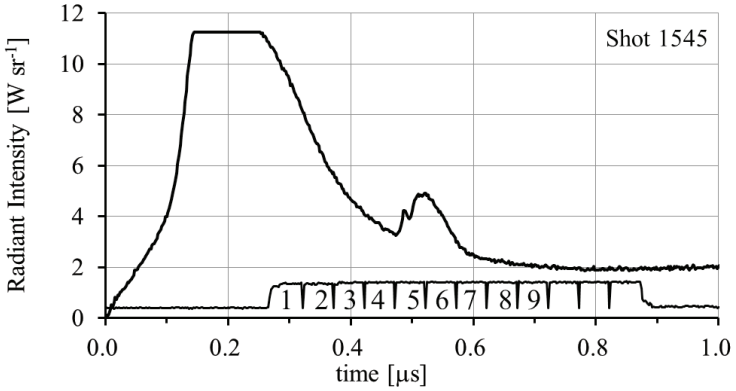

Fig.3. Temporal variation of weighted radiant intensity and exposure timing of ultra-high-speed camera in experiment 1545. The numbers for the exposure timing correspond to the frame numbers in Fig. 4 below. Radiant intensity greater than about 11 W sr^{-1} could not be measured due to the setting of the oscilloscope.

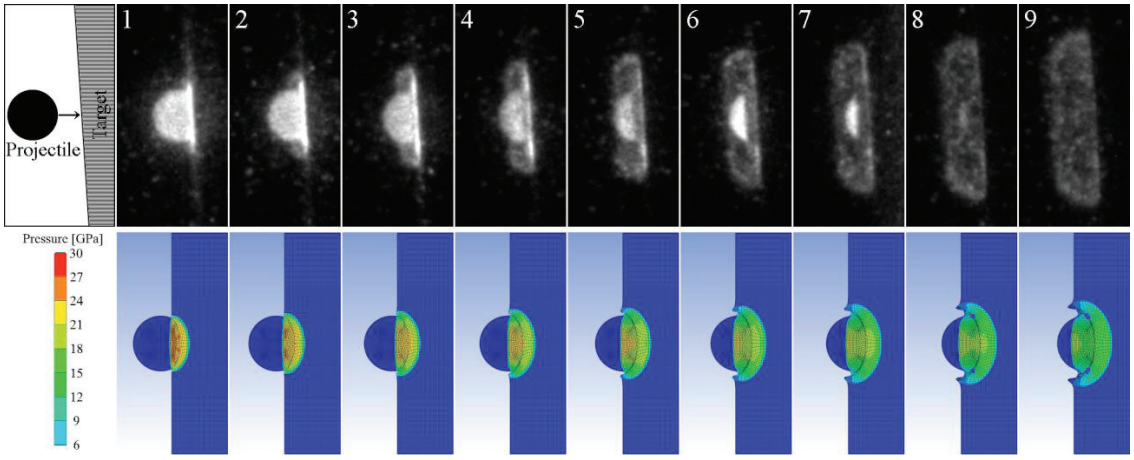

Fig.4. First nine frames obtained by ultra-high-speed camera in experiment 1545. The exposure timings are shown in Fig. 3 (there is 0.05 microsecond between frames). Only the central portion of each frame is displayed. A 7-mm spherical projectile moved from the left to the right horizontally. The target surface is seen edge-on. A result of a numerical simulation is also shown in which the color scale shows the pressure.

We estimated the temperature by shock compression using the simple semianalytical approach of Sugita et al. [8] in a one-dimensional model. Six parameters are necessary for the calculation: C_0 and s used in the simulation by the AutoDyn, the initial density ρ_0 = 1.15 x 10^3 kg m^{-3}, the specific heat at constant volume C_v = 1.2 kJ K^{-1} kg^{-1}, the initial Gruneisen parameter Γ_0 (assumed to be $2s$ - 1 in this calculation), and q = 1 (This means that the Gruneisen parameter is inversely proportional to the density). The estimated temperature is 3600 K for impacts at 7 km s^{-1}.

The source of the observed radiation is assumed to be the shock front of the projectile. The surface area of the shock front can be approximated by the cross-section of the projectile. If the shock front radiates as a blackbody at the temperature T and the radiation is emitted isotropically into half space (2π steradian), the radiant intensity weighted by the relative spectral intensity (Fig. 1) is:

$$I_{\mathrm{PD}} = \frac{\pi(d/2)^2}{2\pi} \cdot \int \frac{2\pi hc^2}{\lambda^5} \left\{ \exp\left(\frac{hc}{\lambda kT}\right) - 1 \right\}^{-1} \cdot f(\lambda) \cdot \mathrm{d}\lambda \tag{2}$$

where d is the projectile diameter, and h, c, and k are, respectively, the Planck constant, the speed of light, and the Boltzmann constant. At 3600 K, I_{PD} is 20 W sr^{-1} and is consistent with the observed radiant intensities shown in Figs. 2 and 3.

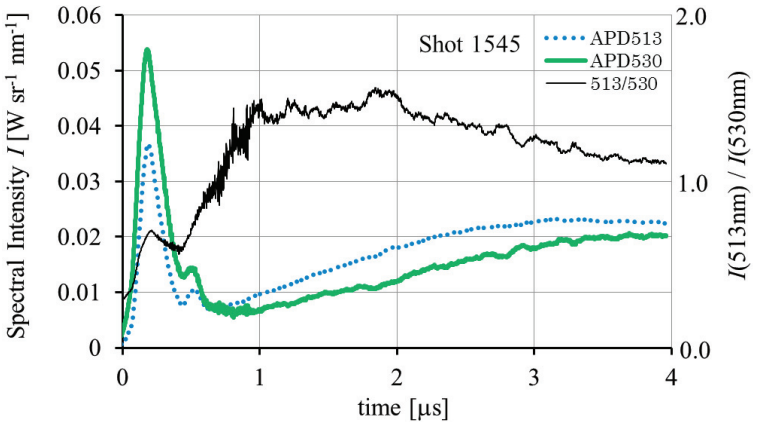

Fig.5. Temporal variation of spectral intensities at 513 nm (blue dotted line) and 530 nm (green thick line) and their intensity ratio (black thin line) in experiment 1545. The so-called C_2 swan band includes the former wavelength but not the latter wavelength. The increase in the ratio indicates an increase in the contribution of C_2 radiation.

A sub-spike was common in our high-velocity impact experiments with Nylon66 spheres. Ultra-high-speed photography showed that the sub-spike is emitted from the Nylon66 projectile (Frame 6 in Fig. 4). On the other hand, nothing special was observed at the time of the sub-spike according to the simulation using AutoDyn (Fig. 4). At present, the origin of this sub-spike is unknown.

5. Conclusion

The source of the noticeable spike in impact flash by Nylon66 projectiles hitting Nylon66 targets is the shock-compressed high-temperature region in the projectile. The radiation is scattered within the translucent projectile and emitted from the surface of the projectile. This spike is not observed with opaque projectiles and is different from the spike observed with the metallic projectiles by Jean and Rollins [1]. On the other hand, it should be observed with other translucent projectiles such as ones made of polyethylene. In the case of transparent projectiles, the visibility of the high temperature region and the amplitude of the spike would depend strongly on the viewing direction, because the total reflection inside the projectile limits the direction in which the radiation can be emitted from the projectile.

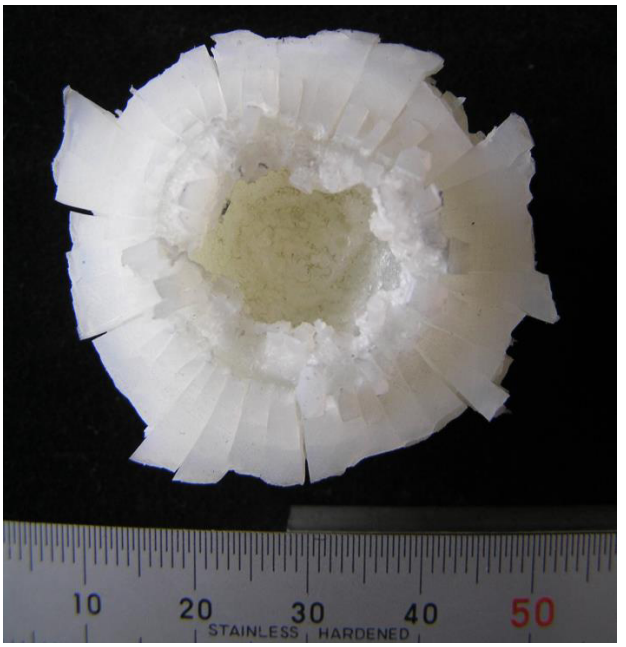

Fig.6. Impact crater formed in a Nylon66 block in experiment 1545. The impacts significantly fragmented the blocks, but craters were always preserved in one of the largest fragments in our experiments. The crater diameter is about 14 mm at the surface and slightly larger inside. Crater depth as measured from the original surface is about 6 mm.

Acknowledgements

This research was supported by the Space Plasma Laboratory, ISAS/JAXA. The ultra-high speed movie images in the figure were taken by NAC Image Technology Inc. We are indebted to E. Sato and N. Kawai for their help in the numerical simulations by the AutoDyn. The authors were supported by the Institute of Low Temperature Science, Hokkaido University for discussion in the workshop on planetary impacts. We thank the two reviewers for their useful comments.

References

[1] Jean, B., Rollins, T. L., 1970. Radiation from Hypervelocity Impact Generated Plasma, AIAA Journal 8, p. 1742.
[2] Ang, J. A., 1990. Impact Flash Jet Initiation Phenomenology, Int. J. Impact Engineering 10, p. 23.
[3] Ernst, C. M., Schultz, P. H., 2007. "Temporal and Spatial Resolution of the Early-Time Impact Flash: Implications for Light Source Distribution", Lunar Planet. Sci. XXXVIII, paper #2353.
[4] http://www.hamamatsu.com/jp/en/product/category/3100/4001/4103/S3071/index.html (last accessed on Jan. 2015).
[5] http://www.hamamatsu.com/jp/en/product/category/3100/4001/4161/C8366/index.html (last accessed on Jan. 2015).
[6] http://www.hamamatsu.com.cn/UserFiles/DownFile/Related/20140308092228880.pdf (last accessed on Jan. 2015).
[7] Marsh, S. P., 1980. LASL Shock Hugoniot Data, Univ. California Press.
[8] Sugita, S., Kurosawa, K., Kadono, T., 2012. "A Semi-Analytical On-Hugoniot EOS of Condensed Matter using a Linear Up-Us Relation", Shock Compression of Condensed Matter, AIP Conf. Proc. 1426, pp. 895-898.